Lawrence Berkeley Laboratory
UNIVERSITY OF CALIFORNIA

ENERGY & ENVIRONMENT DIVISION

To be presented at the Implementation of Computer Procedures and Stress-Strain Laws in Geotechnical Engineering Conference at Virginia Polytechnic Institute, Blacksburg, VA, August 3-6, 1981

MODELING OF STATIC MINING SUBSIDENCE IN A NONLINEAR MEDIUM

J.L. Ratigan and R.E. Goodman

December 1980

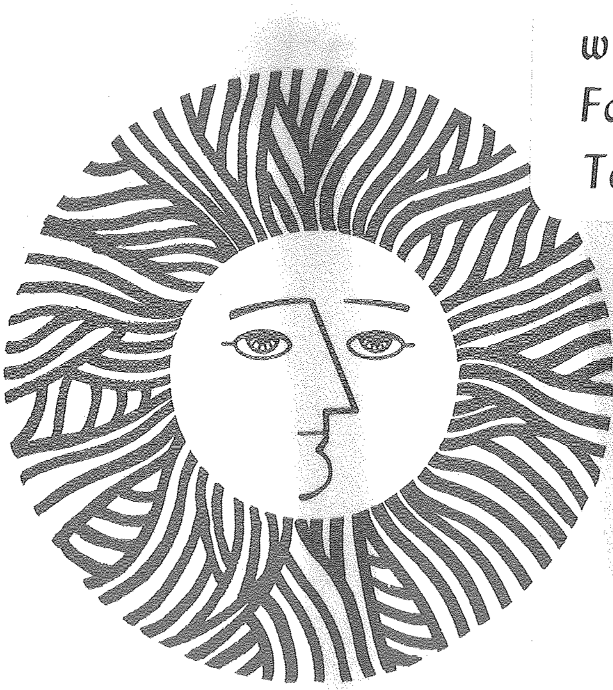

Prepared for the U.S. Department of Energy under Contract W-7405-ENG-48

DISCLAIMER

LBL-11896

MODELING OF STATIC MINING SUBSIDENCE IN A NONLINEAR MEDIUM

Prepared for

Oil Shale Group

Energy and Environment Division
Lawrence Berkeley Laboratory
University of California
Berkeley, California 94720

by

J. L. Ratigan and R. E. Goodman

Department of Civil Engineering
University of California
Berkeley, California 94720

December 1980

This work was supported by the U.S. Department of Energy through the Assistant Secretary for Fossil Energy, Office of Oil Shale, Division of Oil, Gas, and Shale Technology, and the Assistant Secretary for Environment, Office of Environmental Compliance and Overview, Division of Environmental Control Technology under Contract No. W-7405-ENG-48.

SUMMARY

Applications of the conventional finite element method to problems of mining subsidence can result in excessive expense, particularly when nonlinear constitutive stress/strain relations are used for the geological medium. An alternative finite element method is proposed which captures the essential characteristics of subsidence observed both in more sophisticated finite element programs and in the field. The alternative method treats the overburden with classical beam theory with the inclusion of shearing deformation. The nonlinear axial response of the pillars as well as the nonlinear response of any backfill that may be present is also modelled. Flexural and bending modes of deformation are included for the pillar and backfill media with classical beam theory. Shearing deflections are also included for these structural members. The development of the constitutive relations, the implementation of the constitutive relations in the computer program and the numerical algorithm for the problem solution are presented. An example problem in subsidence is presented to illustrate the potential of the computer program. Computer cost for the example problem clearly demonstrates that the alternative method for analysis of subsidence problems deserves consideration.

INTRODUCTION

In the last several decades the finite element method has been applied to numerous mining problems with the gratifying result that designs heretofore arrived upon by trial and error have been improved both from production and safety standpoints. Applications of the finite element method to problems of mining subsidence have been more difficult than applications in other areas due to the lack of obvious multiple geometric symmetry in most mining operations. Thus, finite element models of complex mining arrangements by necessity involve a significant number of degrees of freedom. When direct solution procedures are used to solve the system of linear equations, the solution of practical subsidence problems is often prohibitively expensive due to excessive bandwidths. Although substructuring has alleviated these deficiencies to some degree, substructure technology has not yet permeated the profession.

The purpose of this paper is to present an alternative method of modelling subsidence in a practical and inexpensive manner. The method we shall propose incorporates what we feel to be the salient deformation characteristics of the quasi-static behavior of typical geological materials while maintaining the model design objective of minimizing expense.

The remaining sections of this paper will describe the components of the computer model, the constitutive relationships assumed for the geologic materials, implementation of the constitutive relations, and presentation of an example. A user's manual for the computer program (1) and copies of the deck are available at no cost from the authors.

SUBSIDENCE MODEL ELEMENTS

The program we will present is a nonlinear, two-dimensional, finite element computer program for evaluating static subsidence in a room-and-pillar or a lane-and-pillar configuration with homogeneous and isotropic overburden and homogeneous and isotropic pillars. The basic structural elements within the program are:

- overburden elements
- pillar elements
- room elements

The two-dimensional overburden elements possess six degrees of freedom; specifically, horizontal and vertical translation and rotation at both ends. The behavior of these elements is governed by the slope deflection equations of classical beam theory (2) with the inclusion of shear deflections. The shear deflections are assumed to be invariant with respect to depth.

The pillar elements possess three degrees of freedom, all at the overburden/pillar connection. The pillars may rotate or translate vertically or horizontally. Each pillar is considered to be rigidly attached to a foundation at its lower end (i.e., the lower end may not rotate or translate).

The room elements are similar to the pillar elements. These elements may represent totally excavated cavities by specifying a compressive strength of zero, or they may represent "backfilled" rooms with the appropriate input parameters. Room elements are also considered to be rigidly attached to a foundation at the lower end. Shear deflections for the pillar and room elements are assumed invariant over the width of the room or pillar.

The uniaxial pillar and room elements do not allow for horizontal variations in vertical stress and are only connected structurally via the overburden elements. The response of the pillar and room elements to load is characterized by an initial pore volume decrease and collapse followed by a monotonic strain hardening behavior asymptotically approaching the unconfined compressive strength. Only response to loading in compression is modelled in the program. The pillar and room elements possess infinite stiffness in tension.

CONSTITUTIVE RELATIONSHIPS

The uniaxial stress/strain behavior of the pillar and room elements is illustrated in Figure 1. Region I of the stress/strain curve represents pore volume decrease or microcrack closing and Region II represents strain hardening of the matrix material. Mathematically:

$$\begin{aligned} \sigma &= k(\varepsilon/\varepsilon^*)^N && \text{for} \quad \varepsilon \leq \varepsilon^* \\ \sigma &= (C_o - k)[1 - e^{-\lambda(\varepsilon - \varepsilon^*)}] + k && \text{for} \quad \varepsilon \geq \varepsilon^* \end{aligned} \qquad (1)$$

where σ = uniaxial stress,

ε = uniaxial strain,

C_o = unconfined compressive strength,

ε^*, N, λ = constants determined from laboratory stress/strain data.

Note that the maximum tangent modulus from Eq. (1) occurs at $\varepsilon = \varepsilon^*$. Mathematically, the maximum tangent modulus is:

$$\max \frac{\partial\sigma}{\partial\varepsilon} = \lambda(C_o - k) \quad .$$

From the requirements of stress and stiffness continuity at $\varepsilon = \varepsilon^*$, the following relationship is obtained:

$$k = \frac{\lambda C_o \varepsilon^*}{N + \lambda\varepsilon^*} \quad . \qquad (2)$$

If we consider that the pore structure has collapsed at ε^*, the permanent deformation which would be present from an elastic unloading from ε^* (with a tangent modulus at ε^*), would represent the pre-loading porosity, n.

The resulting expression for pre-loading porosity is obtained:

$$n = \frac{\varepsilon^*(N - 1)}{N} \qquad (3)$$

Bending and flexural deformations within the pillar and room elements are considered to be linear with the applied load and represented with the slope deflection equations. The deformation modulus for these modes of loading is taken to be identical to the tangent modulus from the stress/strain curve of Figure 1 at the present vertical compressive strain.

The load/deformation response of the overburden elements is taken to be linear and constant. Classical beam theory applies with the addition of shear deformations.

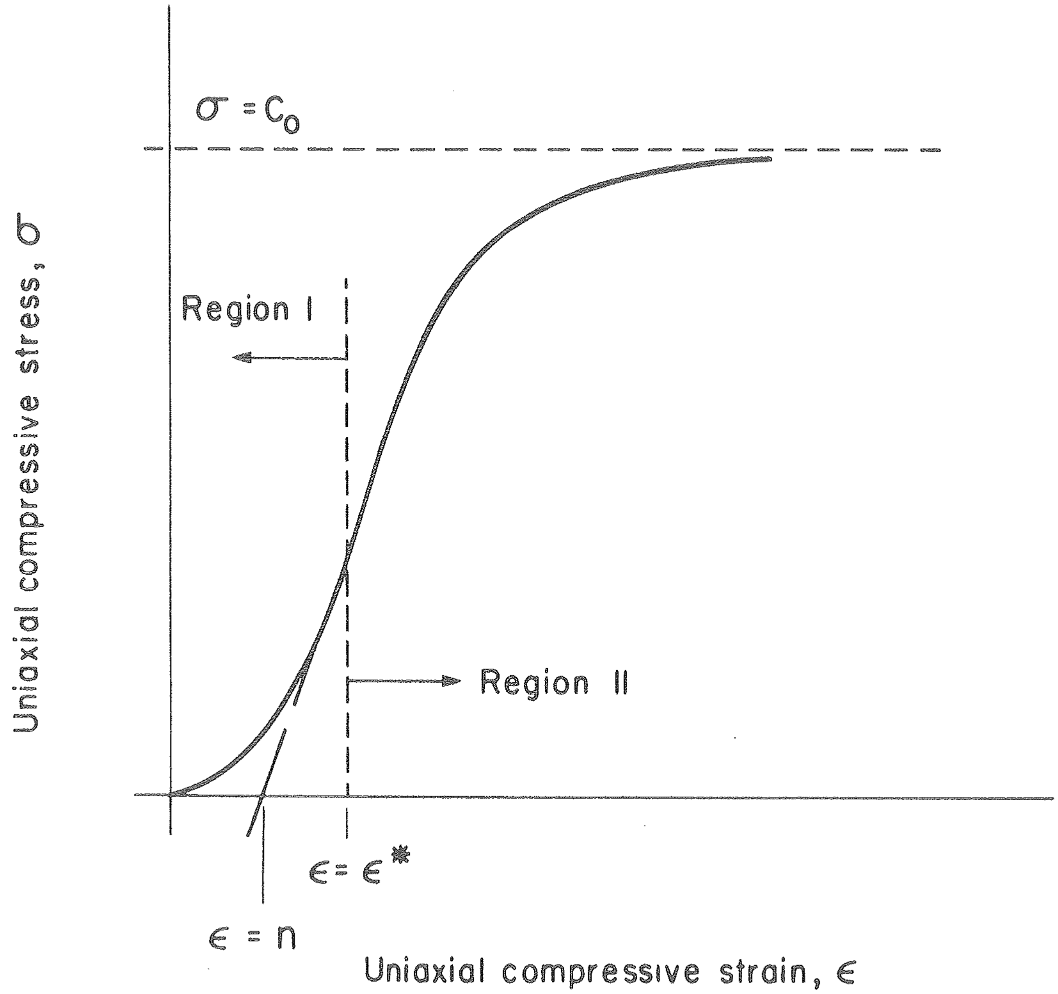

Figure 1. Uniaxial stress/strain response for pillar and room elements.

ELEMENT STIFFNESS MATRICES

This section describes the form of the element stiffnesses. The general form of the force/displacement relations is:

$$[K^e]\{U^e\} = \{F^e\} \tag{4}$$

where $[K^e]$ = the element stiffness matrix,

$\{U^e\}$ = element displacement vector,

$\{F^e\}$ = element force vector.

Discussion of the direct stiffness method and further explanation of Eq. (4) are given elsewhere (2).

<u>Overburden Elements</u>

The forces, displacements, and appropriate sign convention for an overburden element are illustrated in Figure 2. The corresponding form of Eq. (4) is:

$$\frac{E_b I_b}{L(1+2\beta_b)} \begin{bmatrix} \frac{A_b(1+2\beta_b)}{I_b} & & & & & \\ 0 & \frac{12}{L^2} & & & \text{SYMMETRIC} & \\ 0 & -\frac{6}{L} & 4+2\beta_b & & & \\ -\frac{A_b(1+2\beta_b)}{I_b} & 0 & 0 & \frac{A_b(1+2\beta_b)}{I_b} & & \\ 0 & -\frac{12}{L^2} & -\frac{6}{L} & & \frac{12}{L^2} & \\ 0 & \frac{6}{L} & 2-2\beta_b & 0 & -\frac{6}{L} & 4+2\beta_b \end{bmatrix} \begin{bmatrix} X_1 \\ Y_1 \\ \theta_1 \\ X_2 \\ Y_2 \\ \theta_2 \end{bmatrix} = \begin{bmatrix} F_{X_1} \\ F_{Y_1} \\ F_{\theta_1} \\ F_{X_2} \\ F_{Y_2} \\ F_{\theta_2} \end{bmatrix} \tag{5}$$

where E_b = Young's modulus of the overburden element,

I_b = moment of inertia of the overburden element about the z axis,

L = length of the overburden element,

A_b = cross-sectional area of the overburden element,

$\beta_b = 6E_b I_b / L^2 \bar{A}_p G_b = 12 I_b (1 + \nu)/L^2 \bar{A}_p)$,

$\bar{A}_p$ = effective area of the overburden element cross section ($5A_b/6$ for a rectangular cross-section; see any elementary structures text),

G_b = shear modulus of the overburden element,

ν = Poisson's ratio.

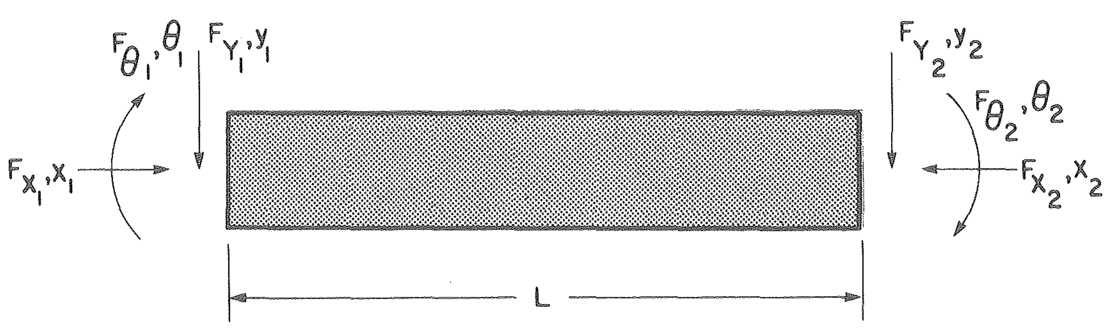

Figure 2 Overburden element forces, displacements, and positive sign convention.

XBL 809-1969

Pillar Elements

The forces, displacements, and appropriate sign convention for a pillar element are illustrated in Figure 3. The force/displacement equations are:

$$
\begin{aligned}
F_{X_p} &= \frac{12E_pI_p}{H_p^{\,3}(1+2\beta_p)} \cdot X_p - \frac{6E_pI_p}{H_p^{\,2}(1+2\beta_p)} \cdot \theta_p \\[2ex]
F_{Y_p} &= k\,A_p\left[\frac{Y_p}{H_p\varepsilon^*}\right]^N && \text{for } \frac{Y_p}{H_p} \le \varepsilon^* \\[2ex]
&= A_p(C_o - k)\left\{1 - \exp\left[-\lambda\left(\frac{Y_p}{H_p} - \varepsilon^*\right)\right]\right\} + k\,A_p && \text{for } \frac{Y_p}{H_p} \ge \varepsilon^* \qquad (6) \\[2ex]
F_{\theta_p} &= -\frac{6E_pI_p}{H_p^{\,2}(1+2\beta_p)} \cdot X_p + \left[\frac{4+2\beta_p}{1+2\beta_p}\right]\frac{E_pI_p}{H_p} \cdot \theta_p
\end{aligned}
$$

where E_p = tangent modulus of the pillar at Y_p/H_p from Eq. (1),

I_p = moment of inertia of the pillar about the z axis,

H_p = height of the pillar,

A_p = cross-sectional area of the pillar,

β_p = shear strain parameter for the pillar [see Eq. (5)].

The following relations between the displacement and forces of the pillar connected to node "i" of an overburden element and the displacements and forces at the overburden element node "i" can be stated as:

$$
\begin{aligned}
X_p &= X_i - \theta_i H_b/2 & F_{X_i} &= F_{X_p} \\
Y_p &= Y_b & F_{X_i} &= F_{Y_p} \\
\theta_p &= \theta_b & F_{\theta_i} &= F_{\theta_p} - H_b \cdot F_{X_p}/2
\end{aligned}
$$

where H_b = the height of the overburden element. Then, Eq. (6) becomes (in terms of the displacements and forces at the ith node):

$$F_{X_i} = \frac{12E_pI_p}{H_p^{\,3}(1 + 2\beta_p)} \cdot X_i - \frac{6E_pI_p}{H_p^{\,2}(1 + 2^{\beta}{}_p)} \left(1 + \frac{H_b}{H_p}\right) \cdot \theta_i$$

$$F_{Y_i} = k\,A_p\left[\frac{Y_i}{H_p\varepsilon^*}\right]^N \qquad \text{for} \quad \frac{Y_i}{H_p} \leq \varepsilon^*$$

$$= A_p(C_o - k)\left\{1 - \exp\left[-\lambda\left(\frac{Y_i}{H_p} - \varepsilon^*\right)\right]\right\} + k\,A_p \qquad \text{for} \quad \frac{Y_i}{H_p} \geq \varepsilon^* \tag{7}$$

$$F_{\theta_i} = -\frac{6E_pI_p}{H_p^{\,2}(1 + 2\beta_p)}\left[1 + \frac{H_b}{H_p}\right] \cdot X_i + \left[\frac{4 + 2\beta_p}{1 + 2\beta_p}\right]\frac{E_pI_p}{H_p}\left[1 + \frac{3H_b}{4H_p}\left(2 + \frac{H_b}{H_p}\right)\right] \cdot \theta_i$$

Equation (7) cannot be written in the form of Eq. (4) directly due to the obvious nonlinearity. In other words, the stiffness of the pillar element depends explicitly on the vertical displacement of the pillar element. The solution procedure or numerical algorithm for the nonlinear equations is discussed later in this paper.

Room Element

The forces, displacements, and appropriate sign convention for the room element are illustrated in Figure 4. The force/displacement equations are identical to those of the pillar elements except that the subscript "p" is replaced with a subscript "r" indicating room material properties and geometry.

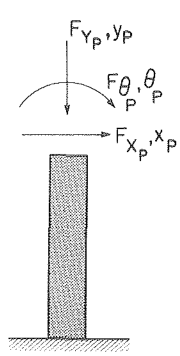

Figure 3 Pillar element forces, displacements, and positive sign convention.

XBL 809-1978

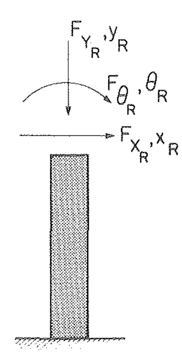

Figure 4 Room element forces, displacements, and positive sign convention.

XBL 809-1970

NUMERICAL ALGORITHM

If the nonlinearity of Eq. (7) did not exist, the element force/displacement relations [Eq. (4)] for each element in a given problem mesh or structure could be merely assembled by means of the direct stiffness method and the resulting set of equations solved. Mathematically:

$$[K]\ \{U\} = \{F\} \tag{8}$$

where $[K] = \sum_e [K^e]$,

$\{U\}$ = 1 by 3N vector of displacements at each of the N nodes,

$\{F\}$ = 1 by 3N vector of forces at each of the N nodes (typically gravitational forces vertically or those due to tectonic in-situ stresses horizontally).

However, due to the nonlinear equations, the solution procedure implied by Eq. (8) is recast as:

$$[K]\{U_i\} = \{F\} - [K^*(U_{i-1})]\ \{U_{i-1}\} \ , \tag{9}$$

where $[K]$ = the stiffness of the structure consisting of the linear portion of the stiffness for all element types,

$\{U_i\}$ = 1 by 3N vector of displacements at iteration i,

$[K^*]$ = the nonlinear part of the stiffness of the structure evaluated for displacements at the $i-1$ iteration.

The linear portion of the pillar and room stiffness is obtained by taking a power series representation of the exponential term of Eq. (7). In this manner, the stiffness components for the room and pillar elements in the [K] matrix are calculated with the maximum tangent modulus (modulus at $\varepsilon = \varepsilon^*$). Therefore, the incremental displacement resulting at each iteration $(U_i - U_{i-1})$ is guaranteed to be a monotonically decreasing function of the number of iterations.

The iteration procedure of Eq. (9) is repeated until a specified number of iterations has been performed or until a maximum relative tolerance on displacement change has been satisfied at every node. Relative tolerance for this program is defined as:

$$\text{Maximum} \quad \left| \frac{U_i^j - U_{i-1}^j}{U_i^j} \right| \qquad j = 1,2,3,\ldots,3N \tag{10}$$

where j = the displacement equation number,

i = the iteration number.

Equation (9) is solved with a direct solver for banded symmetric matrices. Repeated iterations are accomplished by continually re-evaluating the right-hand side of Eq. (9) and performing the appropriate load vector modification and back-substitution for the new displacements.

EXAMPLE PROBLEM

This section illustrates the input and results for a typical example problem and demonstrates how the results may be interpreted. The example problem consists of three lanes 2 m high by 6 m wide located 20 m below the surface (see Figure 5). The lanes or rooms are separated by 4 m wide pillars. By taking advantage of the mechanical symmetry about the vertical plane through the center of the central room, only one half of the configuration need be modeled. The discretization chosen for the evaluation of the subsidence is illustrated in Figure 6. The model is extended in the positive horizontal distance to such a position that the right-hand end will not influence the results near the rooms. Due to the mechanical symmetry, the left-hand side of the model is not free to rotate or translate horizontally. In the region of the rooms, the "coarsest" discretization possible has been used. In the pillar region separating the two modeled rooms, several pillar elements could have been used rather than a single element with an appropriate increase in the number of overburden elements.

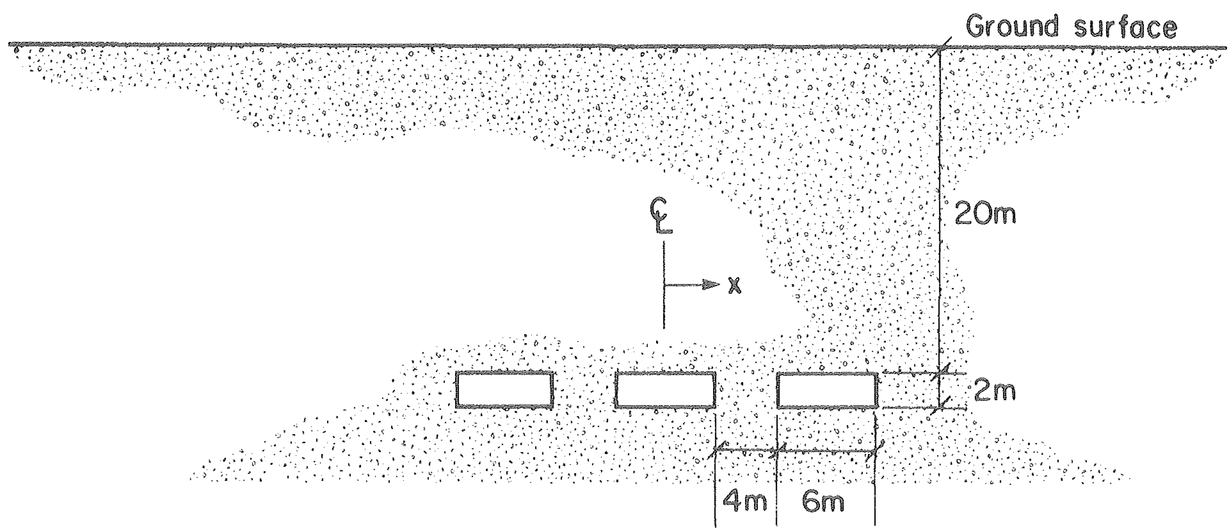

XBL 809-1976

Figure 5. Underground lane section.

Two cases will be presented for this model. Firstly, the model is evaluated with fully excavated rooms (i.e., the room elements have zero strength). Secondly, the rooms will be assumed to be backfilled with a low-strength material. The assumed stress/strain response of the overburden and room and pillar materials is shown in Figure 7 and the remaining material properties are given in Table 1. Note that the pillar and room material has been given a density of zero. Within the program the vertical stress due to the weight of the pillar and room elements is not included in the force/displacement equations. Rather, the mean vertical stress due to the weight of the pillar or room (one half the height of the element times the density) is merely added to the vertical stress induced by the overburden prior to printing of the output.

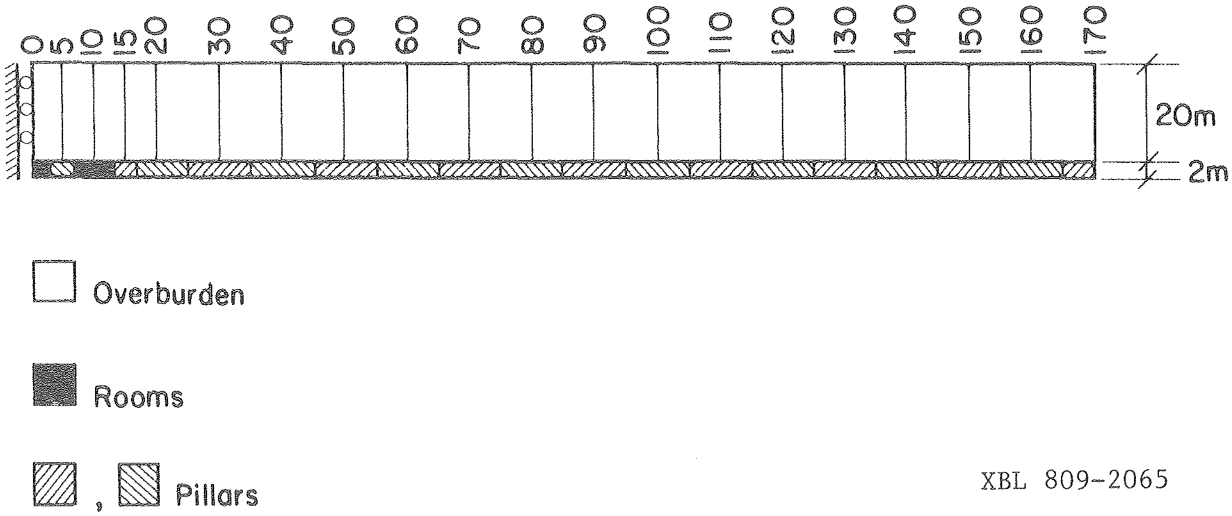

XBL 809-2065

Figure 6. Discretization of underground lanes.

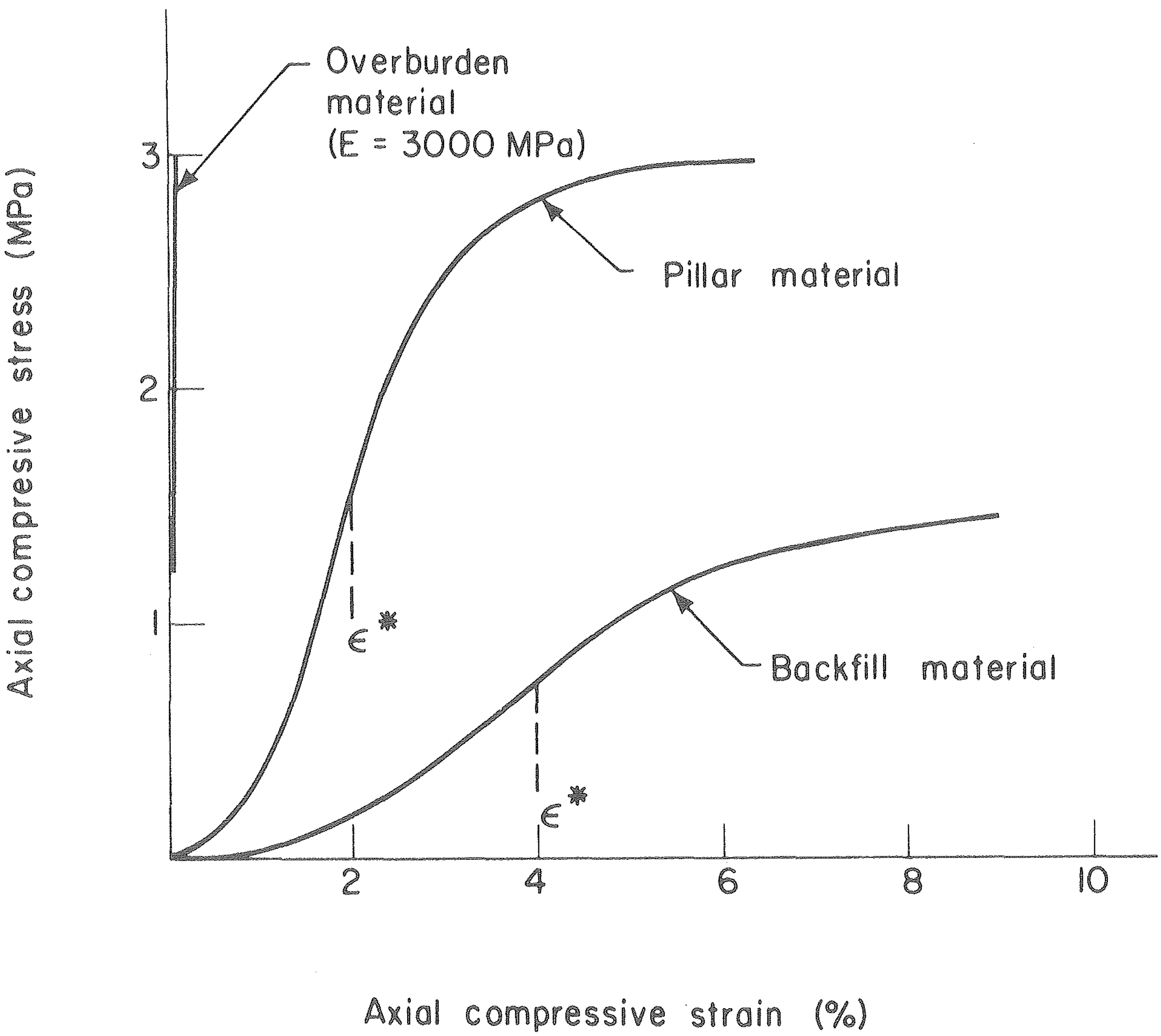

Figure 7 Stress/strain response for model materials. XBL 809-1971

TABLE 1. MATERIAL PROPERTIES FOR EXAMPLE PROBLEM

Region	C_o (MPa)	E (MPa)	G (MPa)	ν	λ	ρ (MPa/m)	N	ε^*
Overburden	-	3000	1200	0.25	-	0.027	-	-
Pillar	3	-	-	0.25	100	-	2	0.02
Room	0/1.5	-	-	0.25	50	-	2	0.04

Since horizontal forces between pillars are not explicitly taken into account in the program, the influence of confinement can be approximated as follows. In pillar elements that will experience little horizontal confinement (elements between rooms), input the uniaxial stress/strain response of the material. In pillar elements that will experience horizontal confinement (elements removed from the rooms), input the stress/strain response of the material at the estimated confining pressure.

The surface displacements for the two cases are shown in Figure 8. The vertical displacements from the computer output are reduced by the amount of the vertical displacement over the "pillar" region without rooms beneath. In other words, the vertical displacement in Figure 8 is that which would result only from the excavation of the rooms. Since the computer output displacements are for nodal locations that are at a depth of one-half the height of the overburden element, the horizontal surface displacements are calculated as:

$$X_s = X_i + \theta_i H_b/2$$

where X_s = horizontal displacement at the top surface of the overburden element,

X_i = horizontal displacement at the nodal location,

θ_i = rotation at the nodal location (positive clockwise).

The three forces which act on the overburden element at each end (see Figure 2) each produce a horizontal stress at the top surface of the overburden element. This horizontal stress at end "1" of the element may be calculated as:

$$\sigma_{X_1} = \frac{F_{\theta_1} \cdot H_b}{2 \cdot I_b} + \frac{F_{X_1}}{A_b} - \frac{F_{Y_1} \cdot H_b \cdot L_b}{4 \cdot I_b}$$

and at end "2" of the element as:

$$\sigma_{X_2} = - \frac{F_{\theta_2} \cdot H_b}{2 \cdot I_b} - \frac{F_{X_2}}{A_b} - \frac{F_{Y_2} \cdot H_b \cdot L_b}{4 \cdot I_b}$$

where compression is taken as positive. The horizontal stress at the top surface of the overburden element will be numerically the same for either end of the element.

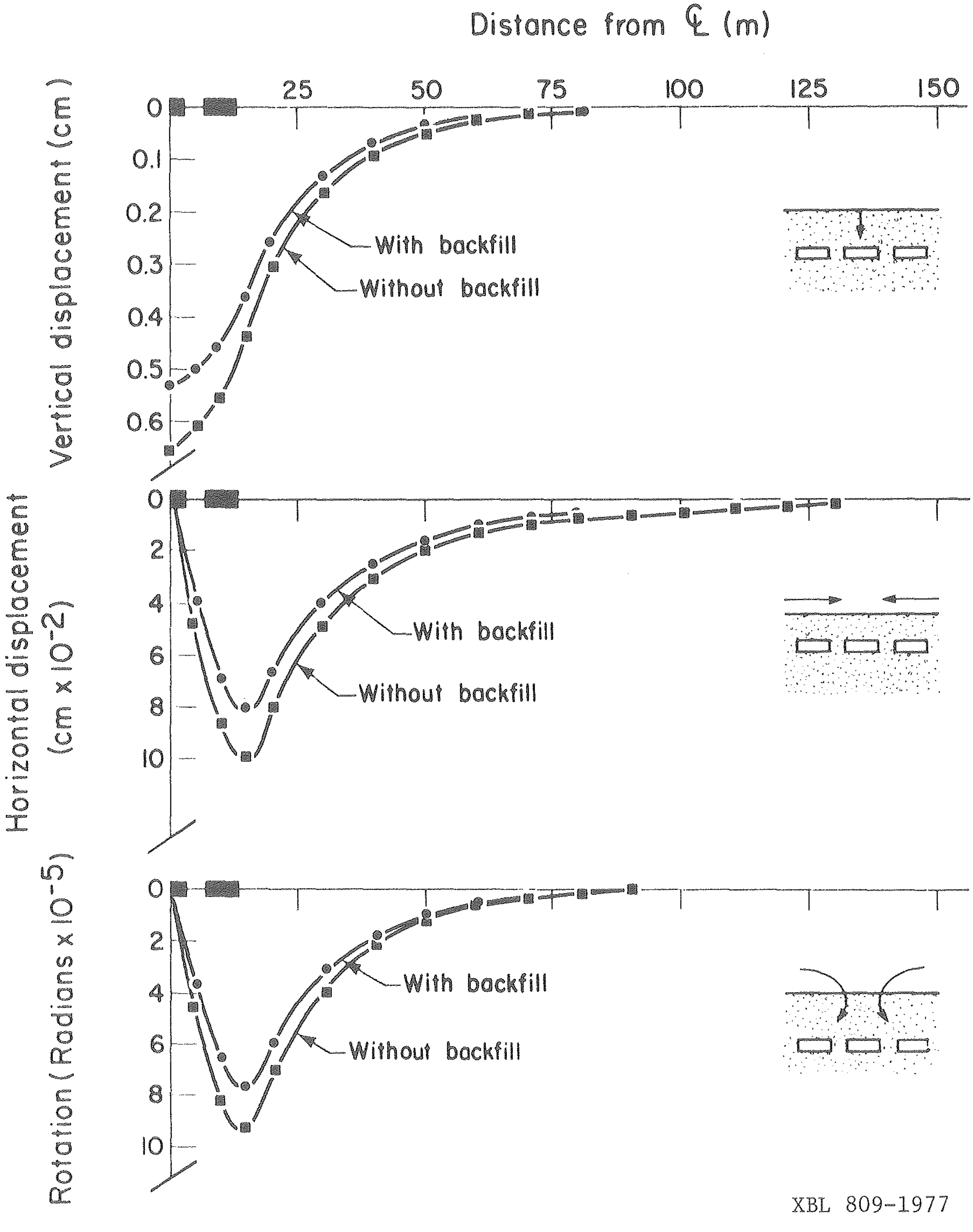

Figure 8. Surface displacements.

The components of the horizontal stress arising from each of the three forces is illustrated in Figure 9 for both cases of the example problem. The superimposed total horizontal stress is shown in Figure 10. Note that a tensile stress of about 0.1 MPa occurs at a distance of about 18 m from the center of the three-room configuration.

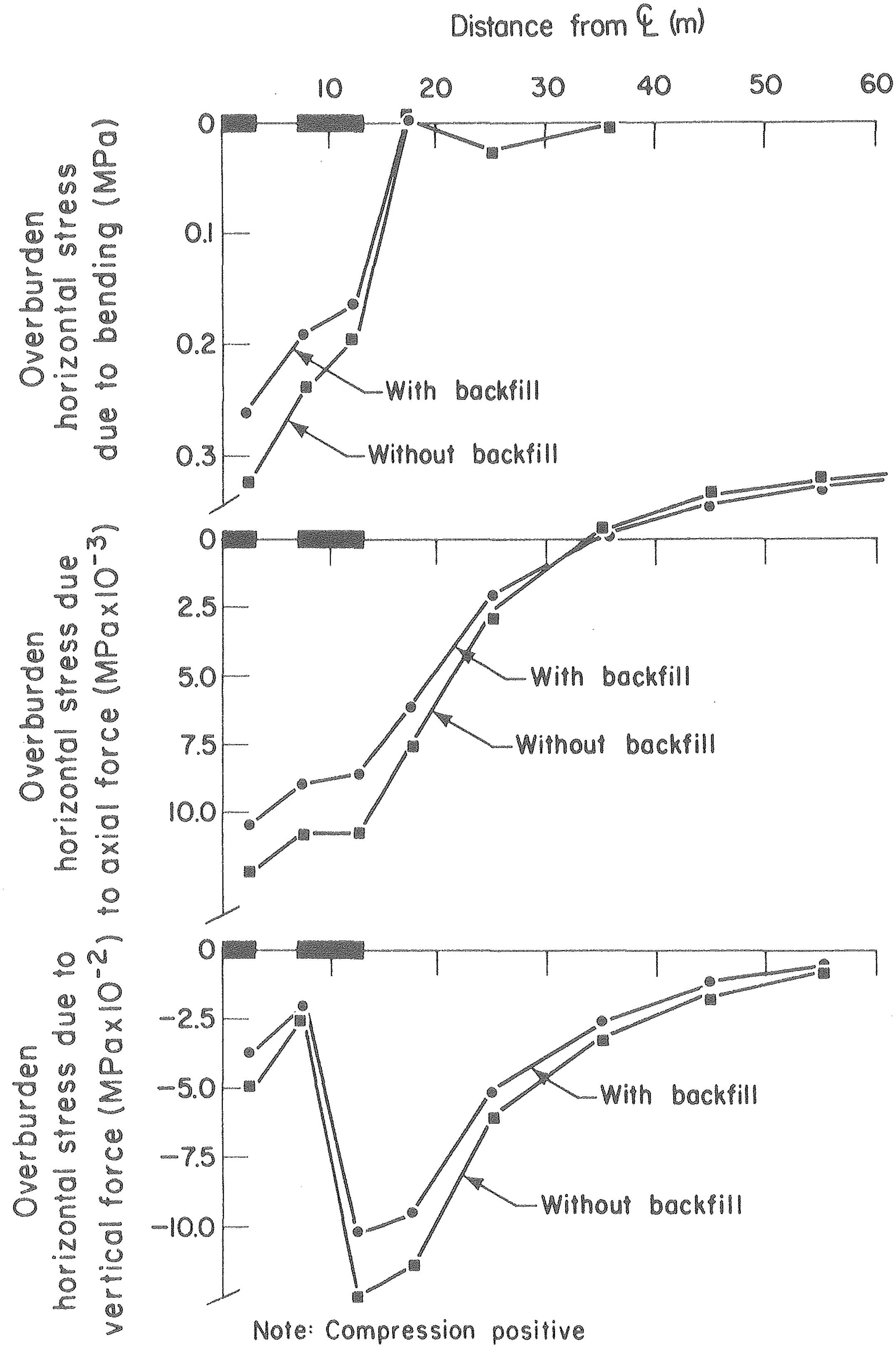

Figure 9. Bending, axial, and flexural stresses in the overburden at the surface.

XBL 809-1972

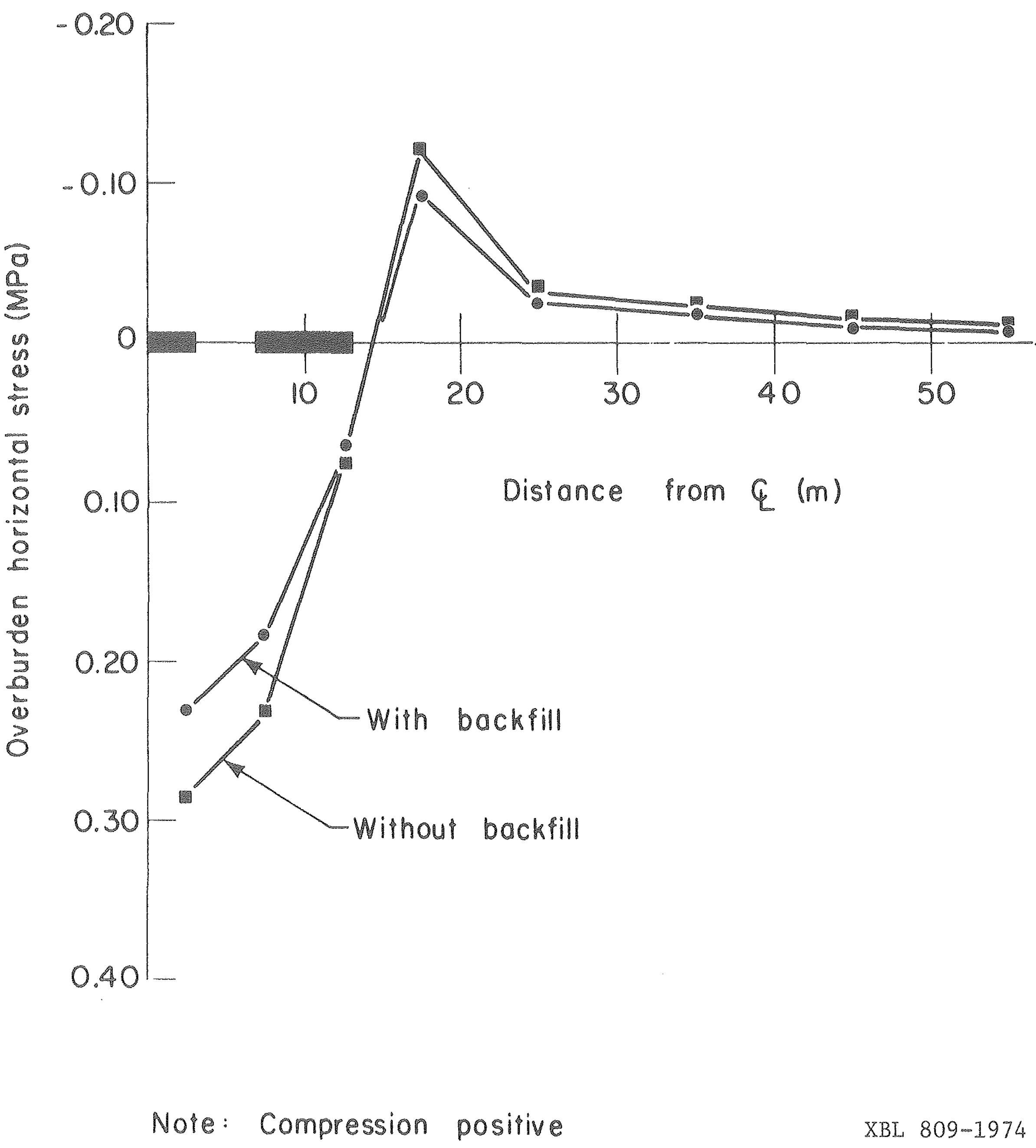

XBL 809-1974

Figure 10. Total horizontal stress at the overburden surface.

In the example cases presented (with and without backfill) 31 and 32 iterations, respectively, were required to achieve a relative tolerance of 10^{-3} on displacements. Each example problem required 0.32 seconds of CPU time on a CDC 7600. The computer program is written with a dynamic storage feature that changes required core for the specific problem at execution time, further reducing the cost of operation. At nominal commercial rates, the cost of executing each example problem would be approximately $0.45.

CONCLUSIONS

An inexpensive alternative to the conventional finite element method has been presented for evaluating subsidence problems in materials with nonlinear stress/strain behavior. Application of the model to a typical subsidence problem has demonstrated the capability to reproduce the essential characteristics of subsidence observed both in more sophisticated finite element calculations and in the field.

ACKNOWLEDGMENTS

The work reported herein was performed for the Oil Shale Group of the Energy and Environment Division of the Lawrence Berkeley Laboratory and was supported by the U.S. Department of Energy through the Assistant Secretary for Fossil Energy, Office of Oil Shale, Division of Oil, Gas, and Shale Technology, and the Assistant Secretary for Environment, Office of Environmental Compliance and Overview, Division of Environmental Control Technology, under Contract No. W-7405-ENG-48.

REFERENCES

1. J. L. Ratigan, "User Information Manual: SUBSID--A Nonlinear, Two-Dimensional Finite Element Program for Static Evaluation of Mining Subsidence," Rep. No. LBL-11356, Lawrence Berkeley Laboratory, Berkeley, California (1980).

2. E. L. Wilson, "CAL78 User Information Manual," Rep. No. UC-SESM 79-1, University of California, Berkeley, Department of Civil Engineering (1978).